frontiers | Frontiers in Plant Science

TYPE Original Research
PUBLISHED 23 February 2023
DOI 10.3389/fpls.2023.1118670

OPEN ACCESS

EDITED BY
Eric Marechal,
UMR5168 Laboratoire de Physiologie Cellulaire Vegetale (LPCV), France

REVIEWED BY
Alexandre Noiriel,
Université Claude Bernard Lyon 1, France
Hubert Schaller,
UPR2357 Institut de biologie moléculaire des plantes (IBMP), France

*CORRESPONDENCE
Martin Potocký
potocky@ueb.cas.cz

SPECIALTY SECTION
This article was submitted to Plant Physiology, a section of the journal Frontiers in Plant Science

RECEIVED 07 December 2022
ACCEPTED 14 February 2023
PUBLISHED 23 February 2023

CITATION
Saddhe AA and Potocký M (2023) Comparative phylogenomic and structural analysis of canonical secretory PLA2 and novel PLA2-like family in plants. *Front. Plant Sci.* 14:1118670. doi: 10.3389/fpls.2023.1118670

Comparative phylogenomic and structural analysis of canonical secretory PLA2 and novel PLA2-like family in plants

Ankush Ashok Saddhe[1] and Martin Potocký[1,2]*

[1]Institute of Experimental Botany of the Czech Academy of Sciences, Prague, Czechia, [2]Department of Experimental Plant Biology, Faculty of Science, Charles University, Prague, Czechia

Plant secretory phospholipase A_2 ($sPLA_2$) is a family of lipolytic enzymes involved in the *sn-2* hydrolysis of phospholipid carboxyester bonds, characterized by the presence of a conserved PA2c domain. PLA_2 produces free fatty acids and lysophospholipids, which regulate several physiological functions, including lipid metabolism, plant growth and development, signal transduction, and response to various environmental stresses. In the present work, we have performed a comparative analysis of PA2c domain-containing genes across plants, focusing on gene distribution, phylogenetic analysis, tissue-specific expression, and homology modeling. Our data revealed the widespread occurrence of multiple $sPLA_2$ in most land plants and documented single $sPLA_2$ in multiple algal groups, indicating an ancestral origin of $sPLA_2$. We described a novel PA2c-containing gene family present in all plant lineages and lacking secretory peptide, which we termed PLA_2-like. Phylogenetic analysis revealed two independent clades in canonical $sPLA_2$ genes referred to as α and β clades, whereas PLA_2-like genes clustered independently as a third clade. Further, we have explored clade-specific gene expressions showing that while all three clades were expressed in vegetative and reproductive tissues, only $sPLA_2$-β and PLA_2-like members were expressed in the pollen and pollen tube. To get insight into the conservation of the gene regulatory network of $sPLA_2$ and PLA_2-like genes, we have analyzed the occurrence of various cis-acting promoter elements across the plant kingdom. The comparative 3D structure analysis revealed conserved and unique features within the PA2c domain for the three clades. Overall, this study will help to understand the evolutionary significance of the PA2c family and lay the foundation for future $sPLA_2$ and PLA_2-like characterization in plants.

KEYWORDS

$sPLA_2$, plant, phylogeny, modelling, pollen, PLA_2-like

1 Introduction

Phospholipases comprise an evolutionarily diverse group of lipolytic enzymes involved in membrane remodeling and hydrolysis of phospholipids into various bioactive lipid derivatives, including free fatty acids (FFA), phosphatidic acid (PA), diacylglycerol (DAG), and lysophospholipids (LPs) (Wang et al., 2012; Chen et al., 2013; Takáč et al., 2019). These lipid derivatives can regulate various physiological functions, including plant growth and development, cellular signaling, and stress management. Based on the site of phospholipid cleavage, phospholipases are classified into three main groups, phospholipase A (PLA), phospholipase C (PLC), and phospholipase D (PLD), each of them exhibiting further variations in the structure, regulation, and catalytic activity. PLA group, which is involved in the hydrolysis of carboxyester bonds from *sn-1*, *sn-2*, or both positions, can be further categorized according to the structural features, catalytic specificity, and calcium (Ca^{2+}) requirement, as PLA_1 (*sn-1* carboxyester bond hydrolysis), secretory PLA_2 (*sn-2* carboxyester bond hydrolysis), and patatin-like PLA_2 (hydrolyze both carboxyester bonds at *sn-1* and *sn-2* positions) (Chen et al., 2013; Takáč et al., 2019). PLA_1 is calcium-independent, has molecular masses ranging from 45–50 kDa, consists of conserved GXSXG motif, and has a catalytic triad (Serine (S), Aspartic acid (D), and Histidine (H)) (Chen et al., 2013). The Arabidopsis genome encodes fourteen PLA_1 gene members that regulate diverse functions such as plant growth and development, shoot gravitropism, production of jasmonic acid, senescence, and ultraviolet B (UV-B) defense signaling (Ishiguro et al., 2001; Kato et al., 2002; Lo et al., 2004; Hyun et al., 2008; Seo et al., 2008; Ellinger et al., 2010; Seo et al., 2011. Similarly, patatin-like PLA (pPLA) is a large enzyme with a patatin domain that serves as a prime active site and requires Ca^{2+} for catalytic activity (Chen et al., 2013). Arabidopsis encodes thirteen pPLA members involved in several physiological processes, including lipid metabolism, signal transduction, cell growth, and plant responses to biotic and abiotic stresses (La Camera et al., 2005; Yang et al., 2007; La Camera et al., 2009; Li et al., 2011; Yang et al., 2012; Li et al., 2013). Patatin-like PLA_2s share a resemblance with the cytosolic animal iPLA2s (group VI) (Balsinde and Balboa, 2005). The other type of phospholipase A_2, secretory PLA_2 ($sPLA_2$) is a small class of enzymes with low molecular masses ranging from 13–18 kDa, N-terminal secretory signal peptide, and PA2c domain (phospholipase A2; EC 3.1.1.4; SMART accession SM00085) that comprises a calcium-binding motif (YGKYCGxxxxGC) and a catalytic site DACCxxHDxC motif (Lee et al., 2005). The secreted $sPLA_2$ variants are the most abundant PLA_2s across nature and are classified into several subgroups I–III, V, IX–XIV. In plants, $sPLA_2$ is evolutionarily grouped into XI IA (PLA_2-β) and XI IB (PLA_2-α) clades (Six and Dennis, 2000). It is involved in diverse physiological functions such as plant growth and development, cell elongation, gravitropism, regulation of auxin, and cellular signaling, and it was also implicated in the responses to biotic and abiotic stress (Takáč et al., 2019; Mariani and Fidelio, 2019).

The first successful plant $sPLA_2$ enzyme purification and characterization attempt has been reported in developing elm seeds (*Ulmus glabra*) (Ståhl et al., 1998). Afterward, $sPLA_2$ encoding cDNAs were isolated from shoots of Oryza sativa and flowers of carnation (*Dianthus caryophyllus*) (Kim et al., 1999; Ståhl et al., 1999). Later, various $sPLA_2$ cDNA, genes, and proteins have been isolated and characterized from several plant species, including *Arabidopsis thaliana*, *Solanum lycopersicum*, *Ricinus communis*, *Nicotiana tabacum*, *Triticum durum*, *Linum usitatissimum*, and *Citrus sinensis* (Dhondt et al., 2000; Fujikawa et al., 2005; Liao and Burns, 2010; Fujikawa et al., 2012; Verlotta et al., 2013; Gupta and Dash, 2017). Arabidopsis genome encodes four sPLA2 isoforms (sPLA2-α, β, γ, and δ), that are categorized into two groups, alpha clade (sPLA2-α) and beta clade (β, γ, and δ). All three members of the beta clade (sPLA2-β, γ, and δ) have been shown to play essential roles in pollen development and pollen tube growth (Kim et al., 2011). Arabidopsis sPLA2-α is required for the trafficking of PIN-FORMED auxin efflux transporters to the plasma membrane and negatively regulates the plant's defense response by repressing the AtMYB30 transcription activity during pathogen infection (Lee et al., 2010; Froidure et al., 2010). At$sPLA_2$-β produces second messengers to enhance light-induced stomatal opening and contributes to cell elongation and shoot gravitropism through the auxin signaling pathway (Lee et al., 2003; Seo et al., 2008).

Despite considerable work on the plant PLA_2, there is little information on comparative structural studies of plants XI IA (PLA_2-β) and XI IB (PLA_2-α) members and no data are available on deep evolutionary comparisons within the plant kingdom (Mansfeld, 2009). Several eukaryotic $sPLA_2$ crystal structures have been elucidated, whereas in plants, only the rice $sPLA_2$ crystal structure has been solved (Guy et al., 2009). It demonstrated that six disulfide bonds stabilize the rice $sPLA_2$ structure, where the N-terminus contains the conserved Ca^{2+}-binding loop, which starts with a short 3_{10}-helix and two short antiparallel β-strands (Guy et al., 2009). Moreover, the C-terminus is folded into three antiparallel α-helices and contains the conserved catalytic histidine and aspartate (HD) residues (Guy et al., 2009). In the present study, we have analyzed the global distribution of $sPLA_2$ members across the plant kingdom. We have identified deep-branching, previously uncharacterized PA2c domain-containing subfamily, termed PLA_2-like, in plants. We analyzed the evolutionary relationship among $sPLA_2$ and PLA_2-Like members, which separated sPLA2-α, β and PLA_2-like into three distinct clades. To get more insight into the expression of the three clades, we have compiled tissue-specific expression data for several angiosperm species, which demonstrated the PLA_2-β members are mainly expressed in the male reproductive tissues. Promoter analysis predicted the presence of tissue, hormone, light, and stress-responsive cis-acting motifs. To uncover conserved structural features in the PA2c fold, we have performed comparative homology modeling of *Amborella trichopoda*, *Arabidopsis thaliana*, and *Nicotiana tabacum* TN90 PLA_2-α, β, and PLA_2-like members. Collectively, this study sheds new light on the sequence and structural evolution of the plant $sPLA_2$ family.

2 Materials and methods

2.1 Plant sPLA$_2$ homologs identification and annotations

A well-annotated Arabidopsis, rice sPLA$_2$-α and β protein sequences were retrieved from Phytozome v13 (https://phytozome.jgi.doe.gov/pz/portal.html) and compiled as initial query sequences. These AtsPLA$_2$ query sequences were used to perform BlastP search against thirty-four plant genomes, including Chlorophyta, Bryophyta, Pteridophyta, Gymnosperm, and Angiosperm species in Phytozome v 13 (https://phytozome.jgi.doe.gov/pz/portal.html), ONEKP database (One Thousand Plant Transcriptomes Initiative, 2019) and NCBI database. Moreover, sPLA$_2$ sequences of several *Nicotiana* species (*N. tabacum* TN90, *N. sylvestris*, and *N. tomentosiformis*) were searched in the SolGenomics database (Mueller et al., 2005). In subsequent rounds of blast searches, PLA2 sequences from bryophytes, and charophyte and chlorophyte algae were also used as queries. Full-length protein and nucleotide sequences were retrieved and manually checked for the presence of an N-terminal secretory peptide, highly conserved PA2c domain in the ScanProsite (https://prosite.expasy.org/scanprosite/), and Interproscan 5 (https://www.ebi.ac.uk/interpro). Further, partial and truncated sequences that suggested incomplete gene predictions were curated using the SoftBerry FGENESH+ gene prediction algorithm (https://www.softberry.com); short and dubious sequences were removed from the dataset. All sPLA$_2$ and PLA$_2$-like sequences were compiled in the table with their genomic information, including gene id, protein length, and chromosomal location (Supplementary Table 1).

2.2 Sequence alignment and phylogenetic analysis

Protein sequences were aligned using the MAFFT E-INS-I algorithm (Katoh and Standley, 2013) in Jalview (Waterhouse et al., 2009). All sequences were manually checked for gaps and non-conserved regions, which were eliminated from the alignment and exported in FASTA file format. The resulting alignment was used to build a sequence logo of the Ca^{2+} binding motif and catalytic motif (https://weblogo.berkeley.edu/logo.cgi) (Crooks et al., 2004). The evolutionary relationship between plant sPLA$_2$ and PLA$_2$-like was inferred using the IQ-TREE algorithm with Maximum likelihood (ML) supported by the ultrafast bootstrap method (1000 replicates). Model finder was performed and the Whelan and Goldman model with Invariable and gamma (WAG+I+G4) was selected as a best model based on the Bayesian information criterion (BIC) score (Minh et al., 2020). The Interactive Tree Of Life (iTOL v5) (https://itol.embl.de/) online tool was used to display and annotate the sPLA$_2$ phylogenetic tree. Likewise, species trees were constructed in NCBI taxonomy and edited in the iTOL server.

2.3 Plant sPLA$_2$ and PLA$_2$-like genes cell and tissue-specific expression analysis

Tissue-specific expression of the sPLA$_2$ and PLA$_2$-like members have been searched in various vegetative (leaf, stem, root, and seeds) and reproductive (flower, anther, pollen, pollen tube, carpels, pistil, ovary, ovule, and egg cells) tissues of Arabidopsis, Amborella, tomato, grape, rice, and maize using the CoNekT database (https://conekt.sbs.ntu.edu.sg/) (Proost and Mutwil, 2018). Gene expression was represented in transcripts per kilobase million (TPM)-based normalization because it can be used for both gene count comparisons within a sample or between samples of the same sample group (Abrams et al., 2019). The expression values were analyzed in the CIMminer one matrix server (discover.nci.nih.gov/cimminer).

Total RNA was isolated from tobacco leaves, roots, buds, flowers, imbibed pollen, germinating pollen grains and growing pollen tubes using Qiagen RNAeasy Kit, and Turbo DNA-free Kit (Applied Biosystems, Waltham, MA, USA) was used for DNA removal. cDNA synthesis was carried out using Transcriptor High Fidelity cDNA Synthesis Kit (Roche, Penzberg, Germany) with anchored-oligo $(DT)_{18}$ primer according to manufacturer's instructions. Semi-quantitative RT-PCR was performed with NtPLA$_2$ gene-specific oligonucleotides 1-6 (Supplementary Table 2) designed to span an intron in the corresponding genomic DNA sequence. Actin7 (Bosch et al., 2005) was used as load control. Amplification conditions were 94°C for 30 sec, 55°C for 30 sec, 68°C for 30 sec and final extension 68°C for 10 min for 28 or 34 cycles.

2.4 Cis-acting elements prediction in sPLA$_2$ and PLA$_2$-like promoters

The promoter regions of sPLA$_2$ and PLA$_2$-like genes (~ 2kbp upstream of the start codon) were retrieved from the Phytozome v13 database. Promoter sequences were then analyzed *via* the PlantCARE server with default parameters (http://bioinformatics.psb.ugent.be/webtools/plantcare/html). The obtained cis-acting elements data were processed using the CIMminer server.

2.5 Prediction of homology models of the sPLA2 and PLA2-like proteins

Homology models of N-terminal truncated peptides signals of *Amborella trichopoda* (ATR0564G112-α; 129 aa, ATR0789G151-β; 118 aa), *Arabidopsis thaliana* (AT2G06925-α; 128 aa, AT2G19690-β; 119 aa), and *Nicotiana tabacum* TN90 (Gene_60450(SS4740)-α; 127 aa, Gene_37244 (SS1768)-β; 117 aa) were obtained through AlphaFold server and also predicted using Robetta server (https://robetta.bakerlab.org/), and RaptorX server (http://raptorx.uchicago.edu/). Moreover, homology models of C-terminal regions (containing PA2c domain) of PLA2-like sequences were predicted for *Amborella trichopoda* (AmTr _scaffold00063; 168 aa), *Arabidopsis thaliana*

(AT4G29070- 145 aa), and *Nicotiana tobacum*TN90 (mRNA_158062; 149 aa). For Robetta and RaptorX, five models of each protein were generated, and the model qualities were compared with the AlphaFold predictions using the SWISS-refinement server (https://swissmodel.expasy.org/assess). MolProbity Score, clash score, Ramachandran scores, and QMEAN were considered to select the best model among all generated predictions. Further, electrostatic potentials for the best models were calculated using APBS web-server (Adaptive Poisson-Boltzmann Solver, https://www.poissonboltzmann.org/) and plotted on the predicted protein structures (Unni et al., 2011). The conserved residues and non-conserved residues were analyzed using the Consurf web-server (https://consurf.tau.ac.il/) for the best models. All the generated models were visualized and edited using the CHIMERA (https://www.cgl.ucsf.edu/chimera/).

3 Results

3.1 Phylogenomic analysis of plant PA2c domain-containing genes revealed an ancient origin of sPLA$_2$ and uncovered a widespread presence of the previously uncharacterized PLA$_2$-like family

To get a deeper insight into the evolution of the plant sPLA2 family, we have selected thirty-four plant genomes representing a diverse and balanced sample of *Viridiplantae*, including algae, bryophytes, lycophytes, pteridophytes, gymnosperms, and angiosperms. We searched within this genome sample for the presence of the sPLA$_2$ homologs, using known dicot and monocot sPLA$_2$ as input and employing various homology-based searches like Blast and HMMER (Figure 1A). We ultimately identified 113 non-redundant canonical plant sPLA$_2$ genes based on the following criteria: the presence of N-terminal signal peptide and PA2c domain with Ca^{2+} binding motif and catalytic HD dyad site. Surprisingly, we also uncovered 37 additional genes coding for proteins that lack the N-terminal signal peptide but contain a well-conserved PA2c domain, including the calcium-binding motif and the catalytic dyad (Supplementary Figure 1, Supplementary Tables 1, 3). The data showed a ubiquitous distribution of both sPLA$_2$ and PLA$_2$-like genes in plants, from unicellular algae to multicellular flowering plants (Figure 1A). Remarkably, the two groups exhibit a clear difference in evolutionary dynamics. PLA$_2$-like orthologs were found as single-copy genes in most diploid species and never exceeded two copies per genome. Two PLA2-like genes were found in either polyploid species (*N. tabacum)* or species that underwent relatively recent whole genome multiplications (*B. rapa*, *G. max*, *P. patens*). This suggests that PLA2-like gene number is under the purifying selection to remain singleton. On the other hand, sPLA$_2$ genes display much wider genomic plasticity, showing gene numbers ranging from one (chlorophyte and streptophyte algae) to twelve (gymnosperm *T. plicata*). This higher evolutionary dynamics of sPLA$_2$ is also apparent for individual plant clades like ferns (two to nine genes) and gymnosperms (four to twelve genes). Within angiosperms, Basal lineages (represented by *A. trichopoda*) seem to contain two sPLA$_2$ genes, while distinct dynamics can be found between dicots (two to six genes) and monocots (four to five genes). Despite the general increase in sPLA$_2$ gene complexity during plant evolution, reductive events can also be observed. In bryophytes, moss *P. patens* and liverwort *M. polymorpha* have two sPLA$_2$ isoforms, whereas only one sPLA$_2$ member was observed in hornwort *A. angustus*. Similarly, just one sPLA$_2$ was retained in the lycophyte *S. moellendorffii* (Figure 1A).

To get more insight into the sequence characteristics of sPLA$_2$ versus PLA$_2$-like subfamilies, we performed multiple sequence alignments of the two groups and analyzed their overall protein sizes, motif occurrences, and the distribution of conserved residues. All sPLA$_2$ sequences have N-terminal signal peptides and range between 90-191 residues, while PLA$_2$-like members range between about 143-320 residues, have extended N- and C-terminal regions, and lack any recognizable signal peptide sequence.

The sequence analysis revealed other notable differences among sPLA$_2$ and PLA$_2$-like members at amino acid levels. Significantly, all sPLA$_2$ members possess twelve cysteine residues forming six disulphide bridges and providing extra structural stability (Mariani and Fidelio, 2019). In contrast, PLA$_2$-like members have only six C residues, possibly forming up to three disulphide bridges (Supplementary Table 3). Moreover, although the highly conserved Ca^{2+} binding loop is present in all members within the PA2c domain, PLA$_2$-like has a subtle variation in Ca^{2+} binding motif with the insertion of an extra residue (YGHYCGxxxxxGK vs YGKYCGxxxxGC) (Figure 1B). Another cysteine loss occurred near the catalytic site where sPLA$_2$-α and β show invariable DxCCxxHDxC motif, whereas PLA$_2$-like has DxCCxxHDxG.

Collectively, our data show a widespread and dynamic occurrence of canonical sPLA$_2$ genes and document a highly conserved, evolutionary-constrained subfamily of non-characterized PLA$_2$-like genes.

3.2 Phylogenetic analysis revealed that sPLA2 and PLA2-like sequences clustered into three deep-branching clades

To shed light on the evolutionary relationships of sPLA$_2$ and PLA$_2$-like families, a curated dataset of 113 sPLA$_2$ and 38 PLA$_2$-like genes was compiled from a diverse set of plants with sequenced genome drafts (Figure 2). It included evolutionary important chlorophytic and streptophytic algal species such as *Chlamydomonas reinhardtii, Volvox carteri, Penium margaritaceum, Klebsormidium nitens, Mesotaenium endlicherianum*, and *Chara braunii*. Moreover, we have included several bryophytes (moss *Physcomitrium patens*, liverwort *Marchantia polymorpha*, and hornwort *Anthoceros angustus*), lycophyte (*Selaginella moellendorffii*), pteridophytes (*Azolla filiculoides*, *Salvinia cucullata*, and *Ceratopteris richardii*), gymnosperms (*Thuja plicata* and *Ginkgo biloba*), Basal angiosperm (*Amborella trichopoda*), and multiple dicots, and monocots species (Figure 2). The sequences were aligned using the MAFFT E-INS-I algorithm, unalignable regions were removed,

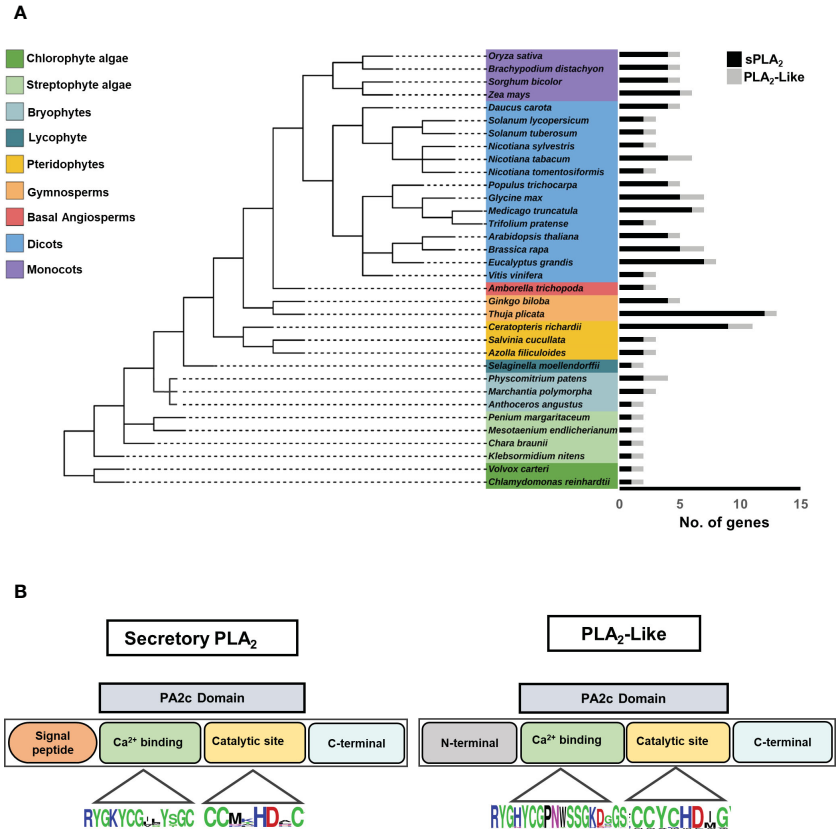

FIGURE 1
(A) Distribution of secretory PLA_2 and PLA_2-like genes in the different plant taxonomic groups, including Algae, Bryophytes, Pteridophytes, Gymnosperms, and Angiosperms. The species tree was elucidated using the NCBI taxonomy database and edited in the Interactive Tree of Life (iTOL) web tool. Each histogram corresponds to the number of $sPLA_2$ and PLA_2-like in each species. Black, histogram-$sPLA_2$; Gray, histogram-PLA2-like genes. **(B)** Schematic representation of PLA_2 protein with N and C terminal, conserved PA2c domain, Ca^{2+} binding motif, and HD catalytic dyad.

and a maximum likelihood (ML) tree was constructed using the IQ-tree software with ultra-fast bootstrap support (Figure 2).

Despite a limited evolutionary signal (due to relatively short sequence lengths), the resulting tree showed clearly that plant PA2c domain-containing genes separated into three well-supported clades. All $sPLA_2$ sequences were clustered into two groups, referred to as sPLA2-α clade and β clade and corresponding to XI-A ($sPLA_2$-β) and XI-B ($sPLA_2$-α) classification of $sPLA_2$ genes (Mansfeld, 2009; Mariani and Fidelio, 2019). Significantly, PLA_2-like members formed a third independent clade, possibly separating $sPLA_2$-α and $sPLA_2$-β (Figure 2). It should be noted that the two canonical clades seem to possess several specific enzymological characteristics, which were best explored in Arabidopsis and elm. Most importantly, $sPLA_2$-α members are show optimal activation by millimolar calcium, while $sPLA_2$-β show maximal activity already at micromolar calcium levels. Compared to $sPLA_2$ members, newly identified PLA_2-like members are large in length (>240 aa), high molecular weight, disordered N-terminal region (~100 aa) without signal peptide, and residual variation in Ca^{2+} binding loop. Moreover, the presence of clear $sPLA_2$-α and $sPLA_2$-β orthologs in gymnosperms and ferns clearly shows that the diversification and stable retention of an α- and β-clade occurred relatively early in land plant evolution. Interestingly, the contrasting $sPLA_2$ distribution in algae and bryophytes (all chlorophyte and streptophyte algae retain 1 $sPLA_2$ isoform clustering in the β-clade, while mosses, liverworts and hornworts possess only α-clade members), suggests that the two clades may have emerged very early in plant $sPLA_2$ evolution, and the single clades were lost in distinct lineages. On the whole, the evolution of the β-clade is clearly under the evolutionary constraint, both in gene number (except for Brassicaceae) and mutation rate (Figure 2). On the other hand, rapidly evolving α-clade is highly expanded in several lineages, including pteridophytes (*C. richardii*), gymnosperms (*T. plicata and G. biloba*), and angiosperms (*E. grandis, P. trichocarpa, G. max*, and *M. truncatula*).

As mentioned above, PLA_2-like clade, which consists of primarily single-copy genes, branched-off from $sPLA_2$ at the earliest stage of green plant evolution, although its presence in green algae was detected universally (Supplementary Table 1). Generally, PLA_2-like phylogeny roughly follows the species evolution with a mutational rate similar to $sPLA_2$-α, suggesting a gradual evolution constrained at the gene number level (Figure 2).

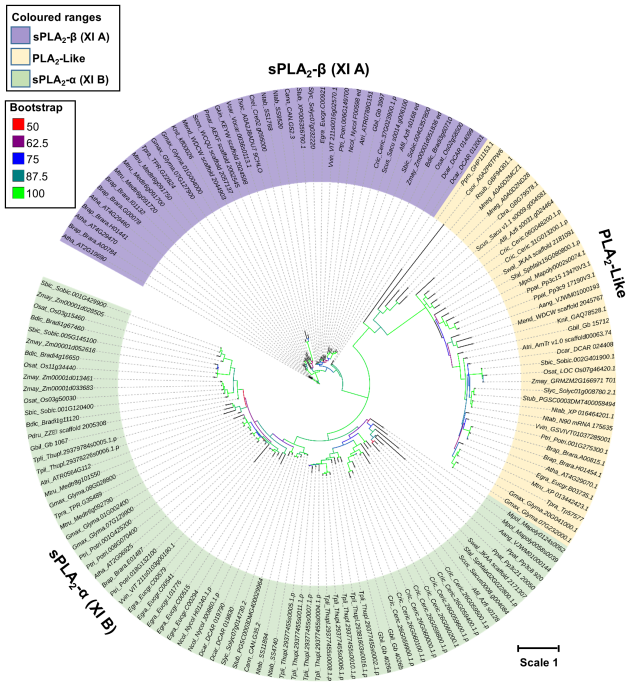

FIGURE 2
Phylogenetic relationships between $sPLA_2$ and PLA_2 -like members were constructed using the Maximum likelihood (ML) with the ultrafast bootstrap method. The evolution Whelan and Goldman model with Invariable and gamma (WAG+I+G4) was selected based on the Bayesian information criterion (BIC) score. Color nodes correspond to the bootstrap support. The scale bar indicates the rates of substitutions/site. Atha, *Arabidopsis thaliana*; Afil, *Azolla filiculoides*; Aang, *Anthocerus angustus*; Atri, *Amborella trichopoda*; Brap, *Brassica rapa*; Bdic, *Brachypodium distachyon*; Cann, *Capsicum annuum*; Crei, *Chlamydomonas reinhardtii*; Csor, *Chlorella sorokiniana*; Cric, *Ceratopteris_richardii*; Dcar, *Daucus carota*; Egra, *Eucalyptus grandis*; Gbil, *Ginkgo biloba*; Gmax, *Glycine max*; Gkin, *Gonatozygon_kinahanii*; Knit, *Klebsormidium nitens*; Mneg, *Monoraphidium neglectum*; Mpol, *Marchantia polymorpha*; Mtru, *Medicago truncatula*; Mend, *Mesotaenium endlicherianum*; Ntab, *Nicotiana tabacum*; Ncol, *Nymphaea colorata*; Osat, *Oryza sativa*; Pdru, *Phylloglossum drummondii*; Ptri, *Populus trichocarpa*; Pmar, *Penium margaritaceum*; Ppat, *Physcomitrium patens*; Ppro; *Pycnococcus provasolii*; Slyc, *Solanum lycopersicum*; Stub, *Solanum tuberosum*; Sbic, *Sorghum bicolor*; Tpli, *Thuja plicata*; Rsub, *Raphidocelis subcapitata*; Scon, *Staurodesmus_convergens*; Swal, *Selaginella_wallacei*; Sfal, *Sphagnumfallax*; Scus, *Salvinia cucullata*; Tsoc, Tetrabaena socialis; Tpra, *Trifolium pratense*; Vvin, *Vitis vinifera*; Vcar, *Volvox carteri*; Zmay, *Zea mays*.

3.3 Global expression analysis shows the overlapping expression of $sPLA_2$ and PLA_2-like genes in the sporophyte and suggests a dominant presence of $sPLA_2$-β clade members in the male gametophyte

To get a comprehensive evolutionary insight into sPLA2 expression, publicly available tissue-specific RNA-Seq data of representative members of eudicots (*A. thaliana*, *S. lycopersicum*, and *V. vinifera*), monocots (*O. sativa* and *Z. mays*), and Basal angiosperms (*A. trichopoda*) have been extracted and arranged clade-specific on the phylogenetic tree (Figure 3A). In total, we analyzed the expression of eleven α-clade members, eight β -clade members, and six PLA_2-like members in four vegetative tissues (leaves, stem, root, and seeds) and ten reproductive tissues (flower, anther, pollen, pollen tube, carpels, pistil, ovary, ovules, and egg cells). The data strongly suggest the existence of conserved clade-specific expression patterns across angiosperms. Members of the $sPLA_2$-α clade in all six analyzed species exhibited significant expression in the vegetative tissues, including leaf, stem, root, and seeds. Notably, while most dicot, monocot and Amborella $sPLA_2$-α members are expressed in the various maternal reproductive tissues, such as flowers, anther, carpels, ovules, and egg cells, they are all conspicuously absent from pollen and pollen tube.

On the other hand, $sPLA_2$-β members across angiosperms showed significant (often the strongest) expression in male gametophytic tissues such as pollen, and pollen tube (and also anther), in addition to variable sporophytic expression. This is well illustrated on the three β-clade and one α-clade Arabidopsis members, where our global expression data analysis is corroborated by earlier RT-PCR and promoter studies (Bahn et al., 2003; Wang et al., 2008). Thus, $AtsPLA_2$-α and β show similar expression in all tissues except male gametophyte, where $AtsPLA_2$-β is significantly expressed. Conversely, $AtsPLA_2$-γ (and to a lesser extent also $AtsPLA_2$-δ) displayed significant expression predominantly in the male gametophyte tissues, including anther, pollen and pollen tube, suggesting that these isoforms might play an essential role in plant reproduction (Bahn et al., 2003; Lee et al., 2005; Wang et al., 2008). The general expression profile of angiosperm PLA_2-like then suggests

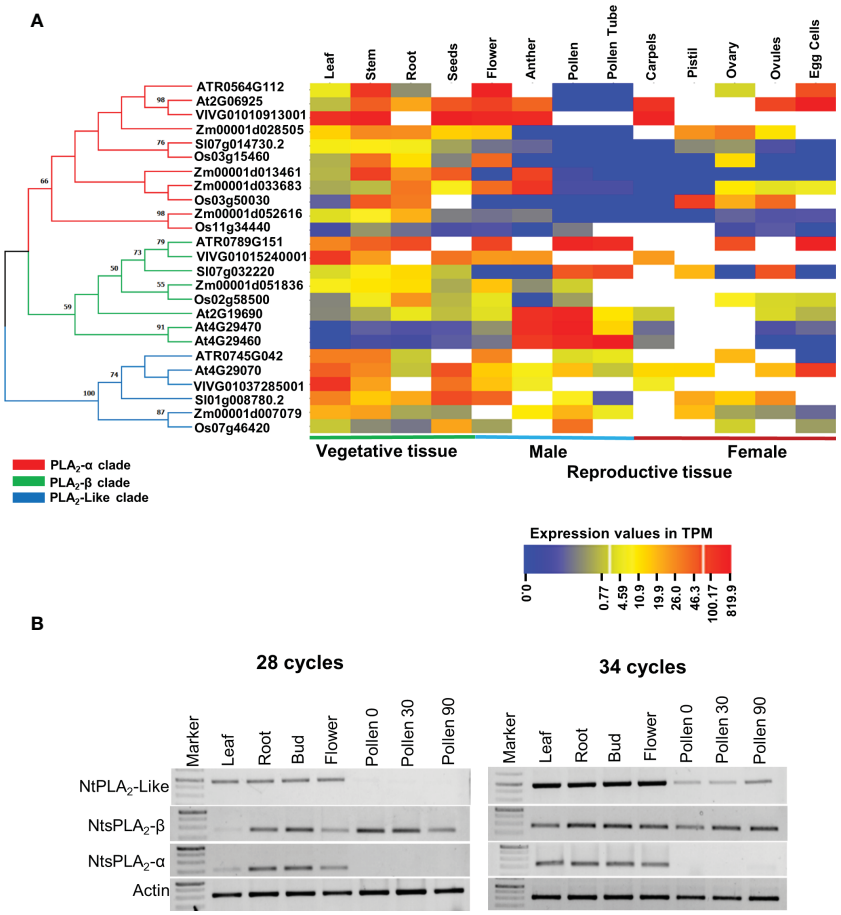

FIGURE 3
(A) Vegetative and reproductive tissue-specific gene expression data of sPLA$_2$ and PLA$_2$-like members were collected for the selected plant species and arranged on a phylogenetic tree. All collected data were exploited to generate the heatmap using the CIMminer web tool. The expression data was represented as a transcript per million (TPM). The phylogenetic relationships between sPLA2- α, β, and PLA$_2$-like members were determined using an ML tree with 100 bootstrap replications in the MEGA X software with the default model. **(B)** Semi-quantitative reverse transcriptase-polymerase chain reaction (RT-PCR) analysis showing the expression of tobacco sPLA2 and PLA2-like members in different tissues and during pollen germination (Pollen30) and pollen tube elongation (Pollen90).

a ubiquitous expression with the highest values typically occurring in the sporophyte and species-diversified expression in the male and female gametophytes (Figure 3A).

To experimentally corroborate these *in silico* studies, we performed a semiquantitative RT-PCR analysis of tobacco PA2c homologs (please note that the sequences of tobacco sPLA$_2$ and PLA$_2$-like homoeologous gene pairs are nearly identical (> 98% nucleotide identity) in tobacco amphidiploid genome and were considered as single cDNAs in the RT-PCR analysis). Analysis of leaf, root, bud, flower, dry pollen, germinating pollen and growing pollen tubes showed that tobacco PA2c genes show expression patterns strongly supporting the RNAseq data on other species, particularly the absence of AtsPLA$_2$-α in pollen and pollen tubes, where PLA$_2$-β is strongly present (Figure 3B). Similarly, tobacco PLA$_2$-like was expressed predominantly in the sporophyte but could be clearly detectable also in the male gametophyte.

Taken together, our comprehensive examination of available transcriptomic data of six angiosperm species and RT-PCR analysis of sPLA$_2$ and PLA$_2$-like genes in tobacco showed evolutionarily conserved expression patterns for the three clades, highlighting their overlapping expression in most sporophytic tissues, and suggesting a significant role for the sPLA$_2$-β clade in pollen.

3.4 Presence of light, stress, and hormone-responsive elements in sPLA$_2$ and PLA$_2$-like promoters across genomes

Having established conserved expression patterns for the three clades of the angiosperm PLA$_2$ family, we next sought to understand their transcription regulatory networks. Therefore, we predicted cis-elements for the promoter sequences of sPLA$_2$ and PLA$_2$-like genes from *Arabidopsis*, wine, rice, and *Amborella* (Figure 4). Various categories of cis-elements were found, including common elements TATA and CAAT box and tissue-specific, light, stress, and hormone-responsive elements.

While no obvious pattern of evolutionarily conserved subset of cis-acting motifs could be attributed to individual sPLA$_2$ or PLA$_2$-like clades, the analysis strongly suggested that specific stress- and hormone-responsive elements are the most significantly

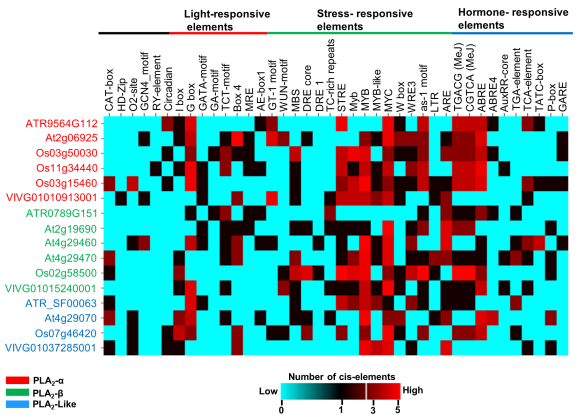

FIGURE 4
In-silico prediction of *cis*-acting elements in the promoter region (5′ upstream region about 2kbp) using PlantCARE database. The number of elements in the promoter regions was depicted by a heatmap using the CIMminer web tool. The color code represents the number of cis-elements in the promoter regions; Cyan- 0 (absent), Red- 5 copies of the element.

overrepresented category in angiosperm sPLA$_2$ and PLA$_2$-like genes. These include abiotic stress-responsive elements, like dehydration-responsive element MBS (TAACTG), Myb (CAACTG), MYB (CAACAG), MYB recognition sites (CAACAG), MYB-like sequence (TAACCA) and MYC (CATTTG).

In addition to the abiotic stress-related elements, motifs implicated in biotic interactions, such as wound-responsive elements W-box (TTGACC), WRE3 (CCACCT), and as-1, were detected in most promoter regions for distinct species. Among those, the WRE3 motif is the most abundant and reported in almost all sPLA$_2$-α and β gene members except *Amborella* and grape genes. W-boxes were found to interact with transcription factors belonging to the WRKY family, regulate defence-related genes, and play a vital role in biotic and biotic stress, senescence and seed dormancy.

Several hormone-responsive elements were documented in the promoter regions, among which abscisic acid-responsive element ABRE (TACGTG) and methyl jasmonate-responsive cis-elements (CGTCA and TGACG) are the most abundant and conserved, particularly within the sPLA$_2$-α clade. On the other hand, ethylene-responsive element ERE (ATTTCAAA), gibberellic acid-responsive elements (GARE: AAACAGA, PA box, and TATC box), auxin responsiveness core element (auxRR: GGTCCAT, TGA elements), show much lower abundance and are scattered among species (Figure 4).

Lastly, many light-responsive cis-elements have been documented in the sPLA$_2$ and PLA$_2$-like promoter regions, including I-box, G box, GATA-motif, GA motif, TCT motif, Box 4, and MRE (MYB binding light responsive elements). The most abundant and conserved motif is G-box (CACGTG), which is involved in the light, abscisic acid, methyl-jasmonate, ethylene and anaerobiosis responses (Sibéril et al., 2001).

Collectively, the abundantly predicted *cis*-acting elements corroborate earlier functions experimentally attributed to selected sPLA$_2$ members and suggest a conserved transcriptional control. Indeed, sPLA$_2$ transcription was activated in response to blue light (Seo et al., 2008), auxin (Scherer, 2002; Lee et al., 2010), abiotic stresses (Chapman, 1998), wound stress and pathogen elicitors (Creelmen and Mullet, 1997; Lee et al., 1997; Laxalt and Munnik, 2002; Ellinger et al., 2010).

3.5 Comparative analysis of sPLA$_2$ and PLA$_2$-like structural models

Despite a wealth of knowledge about PLA$_2$ physiological function, there is limited structural data on the plant sPLA$_2$-α, β, and PLA$_2$-like members, thus impeding our understanding of sPLA$_2$ substrate preferences, interfacial recognition surface (IRS), and catalytic sites. To get better insight into the structural features of sPLA$_2$ and PLA$_2$-like proteins, we thoroughly analyzed structural models predicted for representative members of sPLA$_2$-α, β, and PLA$_2$-like from *Arabidopsis*, tobacco, *Amborella* (Figure 5; Supplementary Figure 2, 3). Since the current databases of automatically-generated structural models include the signal peptide, we generated *de novo* models of the processed sPLA$_2$ forms. Moreover, since the N-terminal extensions in PLA$_2$-like sequences show the characteristics of an intrinsically disordered region, we analyzed only the C-terminal portions. In a pilot analysis, we generated the models using three top-ranked algorithms that are not constrained by existing experimental structures (AlphaFold2_mmseq2 *via* the ColabFold infrastructure, RoseTTAFold, and RaptorX). We assessed them for their folding accuracy based on the Molprobity score, Ramachandran score and Q means plus Z-score criteria (Wang et al., 2016; Waterhouse et al., 2018; Jumper et al., 2021; Baek et al., 2021). Almost universally, AlphaFold-generated models displayed the best criteria and were therefore selected for further analyses (Supplementary Table 4).

Comparative analysis of the final validated models revealed that all display a rather tightly-packed globular structure corresponding to the general sPLA$_2$ fold (Figure 5A; Supplementary Figure 2, 3). Two main structural regions are present across the analyzed species in all sPLA$_2$ and PLA$_2$-like models. The N-terminal part contains mainly a loop region, including a conserved Ca^{2+}-binding loop, and is preceded by two antiparallel beta strands. The C-terminal segment is then represented by three antiparallel α-helices, of which the two first are also present in other secreted PLA$_2$s and contain the conserved catalytic histidine and calcium-coordinating aspartate residues (Guy et al., 2009). Similar structural features were documented in PLA$_2$-like sequences, including the N-terminal loop region with Ca^{2+} binding motif and three antiparallel helices at the C-terminal region with the extended region. Notably, in canonical sPLA$_2$s, the calcium-binding loop and the N-terminal and C-terminal parts are held together by six disulfide cysteine bridges that stabilize the overall structure. However, not all cysteines are

conserved in PLA_2-like sequences, and the structural models suggest that only two cysteine bridges may be retained in PLA_2-like structures, giving them higher conformational flexibility.

Since $sPLA_2$ is an interfacial enzyme interacting with the phospholipid bilayer, we next sought to see the electrostatic potential distribution in all analyzed models that could indicate distinct membrane-binding patterns for separate clades. Our data show that $sPLA_2$-β members in all analyzed species contain positively-charged pockets, which may be involved in anionic lipid binding. On the other hand, all PLA_2-like models lack this feature and produce mostly neutral surfaces. The highest diversity was found within $sPLA_2$-α clade, where significant charge differences can be found between *Arabidopsis*, *Nicotiana* and *Amborella* members (Figure 5B; Supplementary Figure 2, 3). The low evolutionary conservation of the charge distribution was also corroborated by the visualization of evolutionarily conserved surface residues, suggesting that among $sPLA_2$-α, β, and PLA_2-like members, there is rather low conservation beyond the Ca^{2+} binding motif and the catalytic region (Figure 5C).

4 Discussion

4.1 Ubiquitous distribution and ancient divergence record of sPLA2 in plants

Despite the critical importance of PLA_2 documented in higher plants and the availability of detailed molecular information for phospholipases from non-plant organisms, evolution-based knowledge of phospholipase A2 from plants is still meagre. To fill this gap, we have performed a comparative phylogenomic, sequence and structural analysis of the plant's secretory PLA_2 family, along with previously uncharacterized PLA_2-like members. This is the first systematic analysis of the plant family of PA2c domain-containing proteins, covering chlorophyte and streptophyte algal species, bryophytes, lycophyte, pteridophytes, gymnosperms, Basal angiosperm, dicots and monocots. However, the detailed evolutionary history and clade separation of the plant PA2c domain superfamily is murky. Our data demonstrated that one genuine $sPLA_2$ can already be documented in multiple algae species

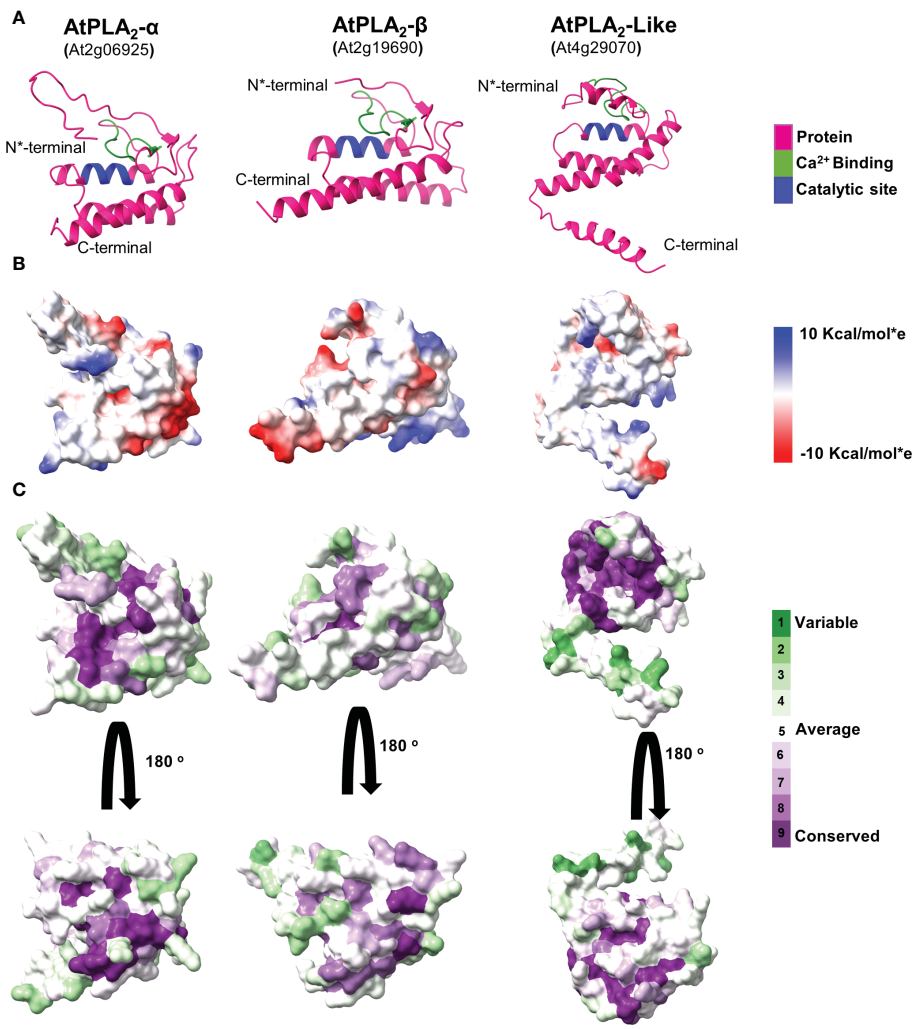

FIGURE 5
A comparative analysis of predicted *Arabidopsis* PLA_2 structural models. **(A)** Cartoon representation of $sPLA_2$-α, PLA_2-β, and PLA_2-like protein models. **(B)** A comparative analysis of the Coulombic electrostatic potential distribution among PLA_2 members, calculated with the ChimeraX software. **(C)** Analysis of conserved residues on the $sPLA_2$ and PLA_2 surfaces, calculated using the Consurf server.

(chlorophytes, charophytes and zygnematophytes), and all canonical algal $sPLA_2$ fall into the XI-A (sPLA2-β) clade. On the other hand, all canonical $sPLA_2$ genes from three main bryophyte groups (hornworts, liverworts, and mosses) belong to the XIB ($sPLA_2$-α) clade, and the simultaneous presence of both clades can be first documented in ferns. Three evolutionary scenarios can explain this diverse distribution: (*i*) $sPLA_2$-β is the ancestral plant form of secretory phospholipase A_2, which through gene duplication and subsequent diversification, gave rise to the $sPLA_2$-α clade during the plant colonization of earth but was secondarily lost in bryophytes and lycophytes; (*ii*) both clades were present already in the common ancestor of chlorophyte and streptophyte algae and were sometimes lost in particular groups; (*iii*) individual $sPLA_2$ clades were subject to the independent horizontal gene transfer events during the evolution of separate Viridiplantae groups. These scenarios are not necessarily mutually exclusive, especially considering the widespread occurrence of horizontal gene transfer in green algae (Ma et al., 2022).

One notable element of plant $sPLA_2$ evolution is the diversity in gene copy numbers for the two clades. The terminal duplication and diversification events of $sPLA_2$ may be attributed to whole-genome duplication (eg. in some bryophyte species), polyploidization or amphidiploidization events (eg. *N. tabacum* or *Z. mays*). In addition, in some pteridophyte and gymnosperm species, $sPLA_2$ underwent massive multiplication. Several hypotheses explain plant gene family expansion besides the whole-genome duplications and hybridization events. Gene families can expand through either segmental, tandem, or retro-transposition (RT) mechanism, but segmental and tandem duplication events were more predominant than RT (Kondrashov, 2012; Panchy et al., 2016). These new paralogs may perform an existing gene function (sub-functionalization) or acquire a novel role (neo-functionalization) (Panchy et al., 2016). These gene duplication mechanisms may often co-occur, as evidenced in the *Eucalyptus grandis,* which genome (n=11) has been shaped by lineage-specific genome duplication events and a high rate of tandem gene duplication (Myburg et al., 2014), leading to the highest number of $sPLA_2$ members found in the analyzed angiosperms. As noted above, most of these within-family multiplication events occurred in the $sPLA_2$-α clade, which is evolving considerably faster than the $sPLA_2$-β clade. The notable exception is Arabidopsis (and the whole *Brassicaceae* clade, Supplementary Table 5, Supplementary Figure 5), where the expansion occurred predominantly in the $sPLA_2$-β clade.

4.2 Is there an evolutionarily conserved role for the sPLA2-β clade in the male gametophyte endomembranes?

Our analysis of the sPLA2 expression revealed that while both -α and -β clades are present in various sporophytic tissues, sPLA2-α genes seem to be absent in the male gametophyte in dicots, monocots and Basal angiosperms (Figure 3A). This contrasts with the expression of the angiosperm $sPLA_2$-β clade members, expressed either exclusively in the pollen and pollen tubes (*Arabidopsis* sPLA2-γ and -δ), or showing the highest expression in the male gametophyte ($sPLA_2$-β from *Arabidopsis*, tomato, monocots, and *Amborella*). Significantly, our high-throughput data analysis is corroborated by the RT-PCR analysis of tobacco $sPLA_2$ members (Figure 3B) and by multiple reports on *Arabidopsis* $sPLA_2$ members (Lee et al., 2005; Kim et al., 2011). Although the split between the two sPLA2 clades occurred before the emergence of sexual reproduction *via* pollen, the presence of only sPLA2-β ortholog already in Amborella pollen and pollen tube suggests that the β-clade is the major sPLA2 in all angiosperms. Indeed, Kim et al. (2011) showed that when all three Arabidopsis PLA2-β clade members were suppressed by RNA interference, pollen development and germination were severely affected. Moreover, lysophosphatidylethanolamine, the product of sPLA2 activity, likely plays a vital role in pollen germination and pollen tube growth (Kim et al., 2011). Significant changes in lysophospholipid levels, including plasma membrane lysophosphatidylethanolamine and lysophosphatidylcholine, were recently described during tobacco pollen germination (Serrano et al., 2022). These findings further corroborate the conserved role of sPLA2 in the male gametophyte. Interestingly, compared to other beta-clade members, *Arabidopsis* sPLA2-γ shows the highest expression in the growing pollen tubes, suggesting that the three different β-clade members in Brassicaceae may have distinct roles during pollen development, germination, and tube growth.

A feature reportedly distinguishing plant sPLA2-α and -β clades is their distinct localization, suggesting that sPLA2-β may act primarily inside the endomembrane system and are not secreted to the apoplast (Fujikawa et al., 2012);. Three Arabidopsis sPLA2-β clade paralogs (β, γ, and δ) localized mainly to the ER and/or Golgi (Seo et al., 2008; Kim et al., 2011) while $sPLA_2$-α localizes either to the apoplast or to the nucleus, depending on the plant status (Froidure et al., 2010; Jung et al., 2012). However, a canonical C-terminal ER-retention signal (KxEL) can be found only in 14 angiosperm $sPLA_2$-β members and is missing even in *Arabidopsis* $sPLA_2$-γ, and -δ. Therefore, the subcellular localization of $sPLA_2$s, particularly the β-clade, might be variable and needs to be determined in other angiosperms.

4.3 The widespread presence of novel, evolutionary-constrained, PLA2-like gene family in plants

While annotating the plant's $sPLA_2$ sequences, we came across a subfamily of proteins with unusually long sequences (~250 aa), that possess a conserved PA2c domain containing both Ca^{2+} binding motif and HD catalytic dyad but lacking a signal peptide, which we termed PLA_2-like. While the presence of the PLA_2-like subfamily was briefly noticed before (Gupta et al., 2017), its phylogenomic distribution and sequence-structural properties were not explored. Our genome-wide analysis demonstrated that at least one PLA_2-like member is consistently present from charophyte algae to higher plants, highlighting an ancient origin. It should be noted that PLA_2-like genes can also be found in chlorophyte algae, but their distribution is patchy, suggesting either frequent losses or horizontal gene transfer in the plant group. Phylogenetically, PLA_2-like sequences clustered into one clade, representing the independent

evolutionary history of PLA2-like members and separating XI-A and XI-B sPLA$_2$s. As noted above, the low gene-copy number of PLA$_2$-like genes is under strong selection, effectively keeping PLA$_2$-like as a single-copy gene in most species. While the putative enzymatic activity of PLA$_2$-like remains obscure, the single-copy status is typically linked with genes often involved in essential metabolic processes and/or the formation of macromolecular complexes. Interestingly, the N-termini of PLA$_2$-like proteins show intrinsically disordered region features, which function in protein-, DNA-, or RNA- binding (Han et al., 2014).

4.4 The angiosperm-conserved involvement of sPLA2 and PLA2-like genes in stress responses and developmental processes

Our analysis of *cis*-acting elements in promoters of evolutionarily-distinct angiosperms species suggested that the transcription of both sPLA$_2$ and PLA$_2$-like genes is regulated by various biotic, abiotic, and developmental stimuli (Figure 4). We have reported different cis-elements (W-box, WRE2, and WUN motif) involved in biotic stress responses, and found several methyl-jasmonate responsive elements in the sPLA$_2$ promoters, further suggesting their active involvement during plant reactions to biotic stresses. The transcriptional activation of sPLA$_2$ genes after a pathogen attack was shown in diverse species such as Arabidopsis (Froidure et al., 2010) and grapevine (Laureano et al., 2018), supporting our *in-silico* analysis. Analogously, sPLA$_2$ promoters have multiple abiotic stress-responsive, abscisic acid-responsive and ethylene-responsive elements in the promoter region, suggesting that sPLA$_2$ may have some regulatory roles during abiotic stresses. Verlotta et al., 2013 characterized durum wheat sPLA$_2$s and assessed their involvement in drought stress (Verlotta et al., 2013). Similarly, Rice sPLA$_2$ also showed a differential expression pattern in response to abiotic stress (Singh et al., 2012).

Besides the involvement in the stress responses, several case studies from distinct species corroborate the conserved transcriptional regulation of sPLA$_2$ after developmental cues (Figure 4). Arabidopsis sPLA$_2$-β is upregulated by auxin and in the curved regions of the peduncle, which were undergoing the gravitropic response (Lee et al., 2003). In *Citrus sinensis*, the sPLA2-α and β genes expression and enzyme activity in leaves and fruits exhibited diurnal rhythmic changes and light regulation, which suggested that diurnal fluctuations in lipophilic second messengers are involved in the regulation of physiological functions (Liao and Burns, 2010).

Very few high-throughput studies described the transcriptional regulation of the *Arabidopsis* PLA$_2$-like gene. Interestingly it was demonstrated among genes with expression changes between pollen germination and tube growth (Wang et al., 2008), and listed among genes involved in *Arabidopsis* acyl lipid metabolism (Beisson et al., 2003). In the present study, we have predicted that PLA2-like members exhibited ubiquitous expression throughout the vegetative and reproductive tissues. In addition, it has light, stress, and hormonal-responsive elements in the promoter region that may be involved in diverse regulatory mechanisms and cellular functions.

4.5 Structural determinants of plant sPLA2 and PLA2-like superfamily

The comparative analysis of structural models for diverse plant sPLA$_2$ and PLA$_2$-like members strongly suggested that there are only subtle differences in the catalytic sites among typical members of sPLA$_2$-α and -β clades. All tested models displayed characteristic sPLA$_2$ features, shared with the experimentally-determined structures of non-plant sPLA$_2$s from groups I, II, X and also rice XI-B sPLA$_2$-namely three α-helices, a short two-stranded β-sheet, and a conserved calcium-binding loop (Dijkstra et al., 1981; Holland et al., 1990; White et al., 1990; Jabeen et al., 2006; Guy et al., 2009). On the other hand, the total conformation (due to the flexibility of N-terminal and C-terminal regions) and charge distribution differ substantially between the two clades or between different phylogenetic groups. For example, the electrostatic charge differences would affect the membrane-binding and protein-binding properties and thus may impact the sPLA$_2$ catalytic functions. Notably, surface charge differences affecting the interactions with negatively-charged phospholipids were also described for non-plant sPLA$_2$ members from groups IIA and X (Quach et al., 2014).

Importantly, template-free modelling of the C-terminal half of PLA$_2$-like proteins suggested a fold similar to canonical sPLA$_2$ structures, including a calcium-binding loop and catalytic dyad. However, the striking difference between the sPLA$_2$ and PLA$_2$-like is the loss of the disulfide bridges, where only four out of twelve Cys residues - forming two disulfide bridges - are conserved in PLA$_2$-like sequences. On the other hand, the two retained disulfide bridges (C140-C167, C166-C192) - which connect helix 1 with the calcium loop and the helices 1 and 2 together - structurally correspond to those that are vital for the PLA$_2$ catalytic activity of porcine PLA$_2$ (C29-C45, C44-C105, Zhu et al., 1995). Therefore, despite the lower number of disulfide bridges retained in PLA$_2$-like structures, PLA$_2$-like members may still possess an enzyme catalytic activity towards lipidic substrates analogous to canonical sPLA$_2$ (Mansfeld, 2009). In addition to the phylogenomic survey of canonical sPLA$_2$ genes, our study may also serve as a call for further enzymological and physiological characterization of the enigmatic PLA$_2$-like gene subfamily.

5 Conclusions

The widespread distribution of canonical sPLA$_2$ and an unexpected presence of novel PLA$_2$-like genes throughout the plant kingdom reflects an ancient sPLA$_2$ origin and possible early split into two separate clades. This points to the conserved functional importance of plant sPLA$_2$. The diverse evolutionary dynamic among the two sPLA$_2$ clades and PLA$_2$-like clade calls for future functional studies, which will be required to shed light on the functional importance of non-*Arabidopsis* β-clade members in

plant reproduction, as well as the molecular characterization of PLA_2-like genes and their involvement in plant cell physiology.

Data availability statement

The original contributions presented in the study are included in the article/Supplementary Material. Further inquiries can be directed to the corresponding author.

Author contributions

MP conceived and guided the study. AAS and MP carried out the analyses. AAS and MP wrote the manuscript. All authors contributed to the article and approved the submitted version.

Funding

This work was supported by the Czech Science Foundation grant GA21-09254S to MP.

Conflict of interest

The authors declare that the research was conducted in the absence of any commercial or financial relationships that could be construed as a potential conflict of interest.

Publisher's note

All claims expressed in this article are solely those of the authors and do not necessarily represent those of their affiliated organizations, or those of the publisher, the editors and the reviewers. Any product that may be evaluated in this article, or claim that may be made by its manufacturer, is not guaranteed or endorsed by the publisher.

Supplementary material

The Supplementary Material for this article can be found online at: https://www.frontiersin.org/articles/10.3389/fpls.2023.1118670/full#supplementary-material

SUPPLEMENTARY FIGURE 1
Sequence alignment of PA2c domain from all analyzed PLA2 proteins - shown separately for sPLA2- α, β **(A)** and PLA2-like **(B)** sequences. Calcium binding motif (red box) and highly conserved catalytic dyad Histidine and aspartic acid (HD) (blue box) are highlighted.

SUPPLEMENTARY FIGURE 2
Predicted models of Nicotiana tabacum sPLA2-α, β, and PLA2-like. **(A)** Cartoon representation of structures. **(B)** Distribution of electrostatic potential on the PLA2 surface.

SUPPLEMENTARY FIGURE 3
Predicted models of Amborella trichopoda PLA2-α, β, and PLA2-like. **(A)** Cartoon representation of structures. **(B)** Distribution of electrostatic potential on the PLA2 surface.

SUPPLEMENTARY FIGURE 4
The positional conservation of cysteine disulfide bridges among canonical $sPLA_2$ members from the -α and -β clade and PLA_2-like proteins. Cysteine residues participating in disulfide bridges are shown in red. Arabidopsis sPLA2 and PLA2-like structural models are shown alongside experimental structure of sPLA2-α from rice.

SUPPLEMENTARY FIGURE 5
Phylogenetic analysis of selected Brassicaceae family $sPLA_2$ members. Phylogenetic tree using *Oryza sativa* $sPLA_2$ members as an outgroup was constructed using the Maximum likelihood (PhyML) with the bootstrap method. The tree analysis was performed using the webserver (https://www.Phylogeny.fr: "One Click" Mode) with default parameters. The scale bar indicates the rates of substitutions/site. Abbreviations: AT, *Arabidopsis thaliana*; AL, *Arabidopsis lyrata;* Ah, *Arabidopsis halleri;* Carub, *Capsella rubella;* Cagra, *Capsella grandiflora;* Brara, *Brassica rapa;* Bol, *Brassica oleracea;* Camar, *Cekile maritima;* Sp, *Schrenkiella parvula.*

SUPPLEMENTARY TABLE 1
List of identified secretory PLA2-α, β, and PLA2-like sequences with their protein length and chromosome locations. (ND – No data, AA – Amino acids).

SUPPLEMENTARY TABLE 2
Primers used for the RT-PCR analysis.

SUPPLEMENTARY TABLE 3
Comparison between *Nicotiana tabacum* Phospholipase A_2 members.

SUPPLEMENTARY TABLE 4
Assessment of sPLA2 and PLA2 structural models.

SUPPLEMENTARY TABLE 5
Analysis of $sPLA_2$ gene family in several *Brassicaceae* species.

SUPPLEMENTARY DATA SHEET 1
Protein sequences of $sPLA_2$ and PLA_2-like analyzed in this study.

SUPPLEMENTARY DATA SHEET 2
Promoter sequences of selected $sPLA_2$ and PLA_2-like genes analyzed in this study.

References

Abrams, Z. B., Johnson, T. S., Huang, K., Payne, P. R. O., and Coombes, K. (2019). A protocol to evaluate RNA sequencing normalization methods. *BMC Bioinf.* 20, 679. doi: 10.1186/s12859-019-3247-x

Baek, M., DiMaio, F., Anishchenko, I., Dauparas, J., Ovchinnikov, S., Lee, G. R., et al. (2021). Accurate prediction of protein structures and interactions using a three-track neural network. *Science* 373 (6557), 871–876. doi: 10.1126/science.abj8754

Bahn, S. C., Lee, H. Y., Kim, H. J., Ryu, S. B., and Shin, J. S. (2003). Characterization of arabidopsis secretory phospholipase A2-gamma cDNA and its enzymatic properties. *FEBS Lett.* 553 (1-2), 113–118. doi: 10.1016/S0014-5793(03)00982-7

Balsinde, J., and Balboa, M. ,. A. (2005). Cellular regulation and proposed biological functions of group VIA calcium-independent phospholipase A2 in activated cells. *Cell. Signal.* 17, 1052–1062. doi: 10.1016/j.cellsig.2005.03.002

Beisson, F., Koo, A. J., Ruuska, S., Schwender, J., Pollard, M., Thelen, J. J., et al. (2003). Arabidopsis genes involved in acyl lipid metabolism. a 2003 census of the candidates, a study of the distribution of expressed sequence tags in organs, and a web-based database. *Plant Physiol.* 132 (2), 681–697. doi: 10.1104/pp.103.022988

Bosch, M., Cheung, A. Y., and Hepler, P. K. (2005). Pectin Methylesterase, a Regulator of Pollen Tube Growth. *Plant Physiol.* 138, 1334–1346. doi: 10.1104/pp.105.059865

Chapman, K. D. (1998). Phospholipase activity during plant growth and development and in response to environmental stress. *Trends Plant Sci.* 3 (11), 419–426. doi: 10.1016/S1360-1385(98)01326-0

Chen, G., Greer, M. S., and Weselake, R. J. (2013). Plant phospholipase a: advances in molecular biology, biochemistry, and cellular function. *Biomol. concepts* 4 (5), 527–532. doi: 10.1515/bmc-2013-0011

Creelman, R. A., and Mullet, J. E. (1997). Oligosaccharins, brassinolides, and jasmonates: nontraditional regulators of plant growth, development, and gene expression. *Plant Cell* 9 (7), 1211–1223. doi: 10.1105/tpc.9.7.1211

Crooks, G. E., Hon, G., Chandonia, J. M., and Brenner, S. E. (2004). WebLogo: a sequence logo generator. *Genome Res.* 14 (6), 1188–1190. doi: 10.1101/gr.849004

Dhondt, S., Geoffroy, P., Stelmach, B. A., Legrand, M., and Heitz, T. (2000). Soluble phospholipase A2 activity is induced before oxylipin accumulation in tobacco mosaic virus-infected tobacco leaves and is contributed by patatin-like enzymes. *Plant J.* 23 (4), 431–440. doi: 10.1046/j.1365-313x.2000.00802.x

Dijkstra, B. W., Kalk, K. H., Hol, W. G., and Drenth, J. (1981). Structure of bovine pancreatic phospholipase A2 at 1.7 Å resolution. *J. Mol. Biol.* 147 (1), 97–123. doi: 10.1016/0022-2836(81)90081-4

Ellinger, D., Stingl, N., Kubigsteltig, I. I., Bals, T., Juenger, M., Pollmann, S., et al. (2010). DONGLE and DEFECTIVE IN ANTHER DEHISCENCE1 lipases are not essential for wound- and pathogen-induced jasmonate biosynthesis: Redundant lipases contribute to jasmonate formation. *Plant Physiol.* 153 (1), 114–127. doi: 10.1104/pp.110.155093

Froidure, S., Canonne, J., Daniel, X., Jauneau, A., Brière, C., Roby, D., et al. (2010). AtsPLA2-alpha nuclear relocalization by the arabidopsis transcription factor AtMYB30 leads to repression of the plant defence response. *P. Natl. Acad. Sci. U.S.A.* 107 (34), 15281–15286. doi: 10.1073/pnas.1009056107

Fujikawa, R., Fujikawa, Y., Iijima, N., and Esaka, M. (2005). Molecular cloning, expression, and characterization of secretory phospholipase A2 in tobacco. *Lipids* 40 (9), 901–908. doi: 10.1007/s11745-005-1450-9

Fujikawa, Y., Fujikawa, Y., Iijima, N., and Esaka, M. (2012). Characterization of secretory phospholipase A2 with phospholipase A1 activity in tobacco, *Nicotiana tabacum* (L.). *Lipids* 47 (3), 303–312. doi: 10.1007/s11745-011-3632-3

Gupta, P., and Dash, P. K. (2017). Molecular details of secretory phospholipase A2 from flax (*Linum usitatissimum l.*) provide insight into its structure and function. *Sci. Rep.* 7 (1), 11080. doi: 10.1038/s41598-017-10969-9

Gupta, P., Saini, R., and Dash, P. K. (2017). Origin and evolution of group XI secretory phospholipase A2 from flax (*Linum usitatissimum*) based on phylogenetic analysis of conserved domains. *3 Biotech.* 7 (3), 1–10. doi: 10.1007/s13205-017-0790-x

Guy, J. E., Ståhl, U., and Lindqvist, Y. (2009). Crystal structure of a class XIB phospholipase A2 (PLA2): rice (*Oryza sativa*) isoform-2 pla2 and an octanoate complex. *J. Biol. Chem.* 284 (29), 19371–19379. doi: 10.1074/jbc.M109.008466

Han, F., Peng, Y., Xu, L., and Xiao, P. (2014). Identification, characterization, and utilization of single copy genes in 29 angiosperm genomes. *BMC Genomics* 15 (1), 504. doi: 10.1186/1471-2164-15-504

Holland, D. R., Clancy, L. L., Muchmore, S. W., Ryde, T. J., Einspahr, H. M., Finzel, B. C., et al. (1990). The crystal structure of a lysine 49 phospholipase A2 from the venom of the cottonmouth snake at 2.0-a resolution. *J. Biol. Chem.* 265 (29), 17649–17656. doi: 10.2210/pdb1ppa/pdb

Hyun, Y., Choi, S., Hwang, H. J., Yu, J., Nam, S. J., Ko, J., et al. (2008). Cooperation and functional diversification of two closely related galactolipase genes for jasmonate biosynthesis. *Dev. Cell* 14 (2), 183–192. doi: 10.1016/j.devcel.2007.11.010

Ishiguro, S., Kawai-Oda, A., Ueda, J., Nishida, I., and Okada, K. (2001). The DEFECTIVE IN ANTHER DEHISCIENCE gene encodes a novel phospholipase A1 catalyzing the initial step of jasmonic acid biosynthesis, which synchronizes pollen maturation, anther dehiscence, and flower opening in *Arabidopsis*. *Plant Cell* 13 (10), 2191–2209. doi: 10.1105/tpc.010192

Jabeen, T., Singh, N., Singh, R. K., Jasti, J., Sharma, S., Kaur, P., et al (2006). Crystal structure of a heterodimer of phospholipase A2 from Naja naja sagittifera at 2.3 A resolution reveals the presence of a new PLA2-like protein with a novel cys 32-Cys 49 disulphide bridge with a bound sugar at the substrate-binding site. *Proteins* 62, 329–337. doi: 10.1002/prot.20708

Jumper, J., Evans, R., Pritzel, A., Green, T., Figurnov, M., Ronneberger, O., et al. (2021). Highly accurate protein structure prediction with AlphaFold. *Nature* 596 (7873), 583–589. doi: 10.1038/s41586-021-03819-2

Jung, J., Kumar, K., Lee, H. Y., Park, Y. I., Cho, H. T., and Ryu, S. B. (2012). Translocation of phospholipase A2α to apoplasts is modulated by developmental stages and bacterial infection in arabidopsis. *Front. Plant Sci.* 3. doi: 10.3389/fpls.2012.00126

Katoh, K., and Standley, D. M. (2013). MAFFT multiple sequence alignment software version 7: improvements in performance and usability. *Mol. Biol. Evol.* 30 (4), 772–780. doi: 10.1093/molbev/mst010

Kato, T., Morita, M. T., Fukaki, H., Yamauchi, Y., Uehara, M., Niihama, M., et al. (2002). SGR2, a phospholipase-like protein, and ZIG/SGR4, a SNARE, are involved in the shoot gravitropism of arabidopsis. *Plant Cell* 14 (1), 33–46. doi: 10.1105/tpc.010215

Kim, J. Y., Chung, Y. S., Ok, S. H., Lee, S. G., Chung, W. I., Kim, I. Y., et al. (1999). Characterization of the full-length sequences of phospholipase A2 induced during flower development. *Biochim. Biophys. Acta* 1489 (2-3), 389–392. doi: 10.1016/s0167-4781(99)00193-1

Kim, H. J., Ok, S. H., Bahn, S. C., Jang, J., Oh, S. A., Park, S. K., et al. (2011). Endoplasmic reticulum- and golgi-localized phospholipase A2 plays critical roles in arabidopsis pollen development and germination. *Plant Cell* 23 (1), 94–110. doi: 10.1105/tpc.110.074799

Kondrashov, F. A. (2012). Gene duplication as a mechanism of genomic adaptation to a changing environment. *Proc. Biol. Sci.* 279 (1749), 5048–5057. doi: 10.1098/rspb.2012.1108

La Camera, S., Balagué, C., Göbel, C., Geoffroy, P., Legrand, M., Feussner, I., et al. (2009). The arabidopsis patatin-like protein 2 (PLP2) plays an essential role in cell death execution and differentially affects biosynthesis of oxylipins and resistance to pathogens. *Mol. Plant Microbe Interact.* 22 (4), 469–481. doi: 10.1094/MPMI-22-4-0469

La Camera, S., Geoffroy, P., Samaha, H., Ndiaye, A., Rahim, G., Legrand, M., et al. (2005). A pathogen-inducible patatin-like lipid acyl hydrolase facilitates fungal and bacterial host colonization in. *Arabidopsis. Plant J.* 44 (5), 810–825. doi: 10.1111/j.1365-313X.2005.02578.x

Laureano, G., Figueiredo, J., Cavaco, A. R., Duarte, B., Caçador, I., Malhó, R., et al. (2018). The interplay between membrane lipids and phospholipase a family members in grapevine resistance against. *Plasmopara viticola. Sci. Rep.* 8 (1), 1–15. doi: 10.1038/s41598-018-32559-z

Laxalt, A. M., and Munnik, T. (2002). Phospholipid signalling in plant defence. *Curr. Opin. Plant Biol.* 5 (4), 332–338. doi: 10.1016/s1369-5266(02)00268-6

Lee, H. Y., Bahn, S. C., Kang, Y. M., Lee, K. H., Kim, H. J., Noh, E. K., et al. (2003). Secretory low molecular weight phospholipase A2 plays important roles in cell elongation and shoot gravitropism in arabidopsis. *Plant Cell* 15 (9), 1990–2002. doi: 10.1105/tpc.014423

Lee, H. Y., Bahn, S. C., Shin, J. S., Hwang, I., Back, K., Doelling, J. H., et al. (2005). Multiple forms of secretory phospholipase A2 in plants. *Prog. Lipid Res.* 44 (1), 52–67. doi: 10.1016/j.plipres.2004.10.002

Lee, O. R., Kim, S. J., Kim, H. J., Hong, J. K., Ryu, S. B., Lee, S. H., et al. (2010). Phospholipase A(2) is required for PIN-FORMED protein trafficking to the plasma membrane in the arabidopsis root. *Plant Cell* 22 (6), 1812–1825. doi: 10.1105/tpc.110.074211

Lee, S., Suh, S., Kim, S., Crain, R. C., Kwak, M. J., Nam, H. G., et al. (1997). Systemic elevation of phosphatidic acid and lysophospholipid levels in wounded plants. *Plant J.* 12 (3), 547–556. doi: 10.1046/j.1365-313x.1997.00547.x

Liao, H.-L., and Burns, J. K. (2010). Light controls phospholipase A2α and β gene expression in citrus sinensis. *J. Exp. Bot.* 61 (9), 2469–2478. doi: 10.1093/jxb/erq083

Li, M., Bahn, S. C., Fan, C., Li, J., Phan, T., Ortiz, M., et al. (2013). Patatin-related phospholipase pPLAIIIδ increases seed oil content with long-chain fatty acids in arabidopsis. *Plant Physiol.* 162 (1), 39–51. doi: 10.1104/pp.113.216994

Li, M., Bahn, S. C., Guo, L., Musgrave, W., Berg, H., Welti, R., et al. (2011). Patatin-related phospholipase pPLAIIIβ-induced changes in lipid metabolism alter cellulose content and cell elongation in arabidopsis. *Plant Cell* 23 (3), 1107–1123. doi: 10.1105/tpc.110.081240

Lo, M., Taylor, C., Wang, L., Nowack, L., Wang, T. W., and Thompson, J. (2004). Characterization of an ultraviolet b-induced lipase in arabidopsis. *Plant Physiol.* 135 (2), 947–958. doi: 10.1104/pp.103.036376

Mansfeld, J. (2009). Plant phospholipases A2: perspectives on biotechnological applications. *Biotechnol. Lett.* 31 (9), 1373–1380. doi: 10.1007/s10529-009-0034-1

Mariani, M. E., and Fidelio, G. D. (2019). Secretory phospholipases A2 in plants. *Front. Plant Sci.* 10. doi: 10.3389/fpls.2019.00861

Ma, J., Wang, S., Zhu, X., Sun, G., Chang, G., Li, L., et al. (2022). Major episodes of horizontal gene transfer drove the evolution of land plants. *Mol. Plant* 15 (5), 857–871. doi: 10.1016/j.molp.2022.02.001

Minh, B. Q., Schmidt, H. A., Chernomor, O., Schrempf, D., Woodhams, M. D., von Haeseler, A., et al. (2020). IQ-TREE 2: New models and efficient methods for phylogenetic inference in the genomic era. *Mol. Biol. Evol.* 37 (5), 1530–1534. doi: 10.1093/molbev/msaa015

Mueller, L. A., Solow, T. H., Taylor, N., Skwarecki, B., Buels, R., Binns, J., et al. (2005). The SOL genomics network: a comparative resource for solanaceae biology and beyond. *Plant Physiol.* 138 (3), 1310–1317. doi: 10.1104/pp.105.060707

Myburg, A. A., Grattapaglia, D., Tuskan, G. A., Hellsten, U., Hayes, R. D., Grimwood, J., et al. (2014). The genome of eucalyptus grandis. *Nature* 510 (7505), 356–362. doi: 10.1038/nature13308

One Thousand Plant Transcriptomes Initiative (2019). One thousand plant transcriptomes and the phylogenomics of green plants. *Nature* 574 (7780), 679–685. doi: 10.1038/s41586-019-1693-2

Panchy, N., Lehti-Shiu, M., and Shiu, S.-H. (2016). Evolution of gene duplication in plants. *Plant Physiol.* 171 (4), 2294–2316. doi: 10.1104/pp.16.00523

Proost, S., and Mutwil, M. (2018). CoNekT: an open-source framework for comparative genomic and transcriptomic network analyses. *Nucleic Acids Res.* 46 (W1), W133–W140. doi: 10.1093/nar/gky336

Quach, N. D., Arnold, R. D., and Cummings, B. S. (2014). Secretory phospholipase A2 enzymes as pharmacological targets for treatment of disease. *Biochem. Pharmacol.* 90 (4), 338–348. doi: 10.1016/j.bcp.2014.05.022

Scherer, G. F. E. (2002). Secondary messengers and phospholipase A2 in auxin signal transduction. *Plant Mol. Biol.* 49, 357–372. doi: 10.1023/A:1015290510483

Seo, Y. S., Kim, E. Y., and Kim, W. T. (2011). The arabidopsis sn-1-specific mitochondrial acylhydrolase AtDLAH is positively correlated with seed viability. *J. Exp. Bot.* 62 (15), 5683–5698. doi: 10.1093/jxb/err250

Seo, J., Lee, H. Y., Choi, H., Choi, Y., Lee, Y., Kim, Y. W., et al. (2008). Phospholipase A2β mediates light-induced stomatal opening in arabidopsis. *J. Exp. Bot.* 59 (13), 3587–3594. doi: 10.1093/jxb/ern208

Serrano, N., Pejchar, P., Soukupová, H., Hubálek, M., and Potocký, M. (2022). Comprehensive analysis of glycerolipid dynamics during tobacco pollen germination and pollen tube growth. *Front. Plant Sci.* 13. doi: 10.3389/fpls.2022.1028311

Sibéril, Y., Doireau, P., and Gantet, P. (2001). Plant bZIP G-box binding factors. modular structure and activation mechanisms. *Eur. J. Biochem.* 268 (22), 5655–5666. doi: 10.1046/j.0014-2956.2001.02552.x

Singh, A., Baranwal, V., Shankar, A., Kanwar, P., Ranjan, R., Yadav, S., et al. (2012). Rice phospholipase a superfamily: organization, phylogenetic and expression analysis during abiotic stresses and development. *PloS One* 7 (2), e30947. doi: 10.1371/journal.pone.0030947

Six, D. A., and Dennis, E. A. (2000). The expanding superfamily of phospholipase A2 enzymes: classification and characterization. *Biochim. Biophys. Acta* 1488 (1-2), 1–19. doi: 10.1016/s1388-1981(00)00105-0

Ståhl, U., Ek, B., and Stymne, S. (1998). Purification and characterization of a low-molecular-weight phospholipase A2 from developing seeds of Elm1. *Plant Physiol.* 117 (1), 197–205. doi: 10.1104/pp.117.1.197

Ståhl, U., Lee, M., Sjödahl, S., Archer, D., Cellini, F., Ek, B., et al. (1999). Plant low-molecular-weight phospholipase A2S (PLA2s) are structurally related to the animal secretory PLA2s and are present as a family of isoforms in rice (*Oryza sativa*). *Plant Mol. Biol.* 41 (4), 481–490. doi: 10.1023/a:1006323405788

Takáč, T., Novák, D., and Šamaj, J. (2019). Recent advances in the cellular and developmental biology of phospholipases in plants. *Front. Plant Sci.* 10. doi: 10.3389/fpls.2019.00362

Unni, S., Huang, Y., Hanson, R. M., Tobias, M., Krishnan, S., Li, W. W., et al. (2011). Web servers and services for electrostatics calculations with APBS and PDB2PQR. *J. Comput. Chem.* 32 (7), 1488–1491. doi: 10.1002/jcc.21720

Verlotta, A., Liberatore, M. T., Cattivelli, L., and Trono, D. (2013). Secretory phospholipases A2 in durum wheat (Triticum durum desf.): Gene expression, enzymatic activity, and relation to drought stress adaptation. *Int. J. Mol. Sci.* 14 (3), 5146–5169. doi: 10.3390/ijms14035146

Wang, S., Li, W., Liu, S., and Xu, J. (2016). RaptorX-property: a web server for protein structure property prediction. *Nucleic Acids Res.* 44 (W1), W430–W435. doi: 10.1093/nar/gkw306

Wang, G., Ryu, S., and Wang, X. (2012). Plant phospholipases: An overview. *Methods Mol. Biol.* 861, 123–137. doi: 10.1007/978-1-61779-600-5_8

Wang, Y., Zhang, W. Z., Song, L. F., Zou, J. J., Su, Z., and Wu, W. H. (2008). Transcriptome analyses show changes in gene expression to accompany pollen germination and tube growth in arabidopsis. *Plant Physiol.* 148 (3), 1201–1211. doi: 10.1104/pp.108.126375

Waterhouse, A., Bertoni, M., Bienert, S., Studer, G., Tauriello, G., Gumienny, R., et al. (2018). SWISS-MODEL: homology modelling of protein structures and complexes. *Nucleic Acids Res.* 46 (W1), W296–W303. doi: 10.1093/nar/gky427

Waterhouse, A. M., Procter, J. B., Martin, D. M., Clamp, M., and Barton, G. J. (2009). Jalview version 2–a multiple sequence alignment editor and analysis workbench. *Bioinformatics* 25 (9), 1189–1191. doi: 10.1093/bioinformatics/btp033

White, S. P., Scott, D. L., Otwinowski, Z., Gelb, M. H., and Sigler, P. B. (1990). Crystal structure of cobra-venom phospholipaseA2 in a complex with a transition-state analogue. *Science* 250 (4987), 1560–1563. doi: 10.1126/science.2274787

Yang, W., Devaiah, S. P., Pan, X., Isaac, G., Welti, R., and Wang, X. (2007). AtPLAI is an acyl hydrolase involved in basal jasmonic acid production and arabidopsis resistance to botrytis cinerea. *J. Biol. Chem.* 282 (25), 18116–18128. doi: 10.1074/jbc.M700405200

Yang, W. Y., Zheng, Y., Bahn, S. C., Pan, X. Q., Li, M. Y., Vu, H. S., et al. (2012). The patatin-containing phospholipase a pPLAIIα modulates oxylipin formation and water loss in *Arabidopsis thaliana*. *Mol. Plant* 5 (2), 452–460. doi: 10.1093/mp/ssr118

Zhu, H., Dupureur, C. M., Zhang, X., and Tsai, M. D. (1995). Phospholipase A2 engineering. the roles of disulfide bonds in structure, conformational stability, and catalytic function. *Biochemistry* 34 (46), 15307–15314. doi: 10.1021/bi00046a040